AD-A266 744

:UMENTATION PAGE

Form Approved
OMB No. 0704-0188

2. REPORT DATE	3. REPORT TYPE AND DATES COVERED
May 5, 1993	FINAL - 3/1/90-2/28/93

4. TITLE AND SUBTITLE
SEARCH FOR FAR INFRARED RADIATION FROM OPTICALLY PUMPED DEFECT MODES

5. FUNDING NUMBERS
DAAL03-90-G-0040

6. AUTHOR(S)
A. J. SIEVERS

7. PERFORMING ORGANIZATION NAME(S) AND ADDRESS(ES)
CORNELL UNIVERSITY
LABORATORY OF ATOMIC & SOLID STATE PHYSICS
CLARK HALL
ITHACA, NEW YORK 14853-2501

8. PERFORMING ORGANIZATION REPORT NUMBER

9. SPONSORING/MONITORING AGENCY NAME(S) AND ADDRESS(ES)
U. S. Army Research Office
P. O. Box 12211
Research Triangle Park, NC 27709-2211

10. SPONSORING/MONITORING AGENCY REPORT NUMBER
ARO 26996.8-PH

11. SUPPLEMENTARY NOTES
The view, opinions and/or findings contained in this report are those of the author(s) and should not be construed as an official Department of the Army position, policy, or decision, unless so designated by other documentation.

12a. DISTRIBUTION/AVAILABILITY STATEMENT
Approved for public release; distribution unlimited.

12b. DISTRIBUTION CODE

13. ABSTRACT *(Maximum 200 words)*

Five different experimental studies are described.

(a) Hole burning in chalcogenide glasses: The quantitative form of the hole relaxation depends solely on the average coordination number of the glass independent of chemical composition.

(b) PIRSH Burning of Tb^{3+} in Alkaline Earth Fluoride Crystals: These PIRSHs in "glassy" crystals display the characteristic properties of spectral holes burned in true glasses.

(c) NO_2^- Ions in Alkali Halides: Four different kinds of vibrational hole burning have been carried out: (1) the hole and antihole in the same absorption line, (2) the antihole removed in frequency from the inhomogeneously broadened line, (3) multiple antiholes and (4) the burning at one vibrational mode frequency while monitoring the persistent changes produced in the other internal (IR) or external (FIR) modes with a high resolution FT interferometer.

(d) Calculations and Simulations of Vibrational Solitons in Crystals: The stationary localized mode results for perfect anharmonic crystals are reminiscent of the defect induced local modes studied in the harmonic approximation.

(e) KI:Ag^+ Vibrational Dynamics: First Evidence for Vibrational Solitons: The silver ion in KI is the most thermally unstable lattice-defect combination known. It may result from localised anharmonic modes being released into the lattice.

14. SUBJECT TERMS
persistent IR hole burning, crystals, glasses, rare earth ions, molecules, NO_2^-, FT interferometer, diode lasers, vibrational solitons, KI:Ag^+.

15. NUMBER OF PAGES

16. PRICE CODE

17. SECURITY CLASSIFICATION OF REPORT	18. SECURITY CLASSIFICATION OF THIS PAGE	19. SECURITY CLASSIFICATION OF ABSTRACT	20. LIMITATION OF ABSTRACT
UNCLASSIFIED	UNCLASSIFIED	UNCLASSIFIED	UL

SEARCH FOR FAR INFRARED RADIATION FROM OPTICALLY PUMPED DEFECT MODES

FINAL REPORT

A. J. SIEVERS

MAY 5, 1993

U. S. ARMY RESEARCH OFFICE

GRANT DAAL03-90-G-0040

CORNELL UNIVERSITY

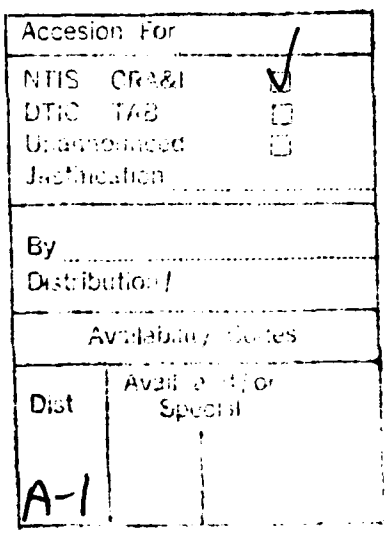

THE VIEW, OPINIONS, AND/OR FINDINGS CONTAINED IN THIS REPORT ARE THOSE OF THE AUTHOR AND SHOULD NOT BE CONSTRUED AS AN OFFICIAL DEPARTMENT OF THE ARMY POSITION, POLICY, OR DECISION, UNLESS SO DESIGNATED BY OTHER DOCUMENTATION.

Table of Contents

I SUMMARY

The studies described here, which are an outgrowth of our previous work on persistent IR spectral hole burning and the high resolution far IR spectroscopic properties of solids, pertain mainly to understanding the cause of the anomalous thermal and vibrational energy transfer properties which we have found in some crystalline and glassy solids. The anomalies we have uncovered are not simply associated with some individual complexity of a particular system but instead indicate that there is a common cause, that is, a characteristic but as yet not clearly specified way by which a variety of systems may transfer vibrational energy.

The evidence is not all in but it appears that, in addition to plane wave vibrational excitations of the lattice, there may be localized vibrational solitons which can move through the crystal. Because the presence of these localized excitations relies on crystal anharmonicity in the pure crystal, they could appear when some region of the lattice was placed under extreme conditions, for example, immediately after an optically induced S –> P state electronic or molecular vibration transition or after a Mössbauer recoil. The presence of point or line defects in the solid would provide a natural low temperature habitat for these localized excitations. The dynamics should be similar to those of localized defect modes, as calculated in the harmonic approximation, except for some important differences. If defects are close enough together then these localized excitations could tunnel or hop from one site to another. As the temperature of the lattice is increased these excitations could escape from the defect neighborhood since they also are allowed in the perfect crystal. One result would be a completely different local mode spectrum.

If these localized excitations do exist then it becomes possible to interpret some solid state phenomena in a new way. For example, in glasses and glassy crystals the tunneling of such vibrational solitons (vibrational energy) from place to place is at least as easy to understand as the likelihood that "groups of atoms" produce a similar tunneling signature in all amorphous solids. One end result would be that the persistent spectral hole burning observed so far for all glass matrices would stem from the tunneling of vibrational solitons near the probe center.

The occurrence of an energy gap law (log of the decay rate ~ $-\Delta E/E_{phonon}$) to describe the non radiative energy decay rate of rare earth ion inner shell electronic excited states in solids and the apparent absence of a similar law for more strongly phonon coupled electronic states or for molecular vibrational states with the same transition energy ΔE is another example. Small amplitude photon induced changes excite phonons which move away from the site at the velocity of sound while large amplitude ones generate vibrational solitons which may move away at ~ 1/20 th the velocity of sound or may not move at all and hence produce local hot spots. In this picture the two vibrational limits produce completely different energy transfer dynamics because the underlying anharmonic solid is fundamentally bistable.

In the next section of the final report we briefly review our major experimental measurements obtained during the last three years.

(a) Hole burning in chalcogenide glasses: Persistent IR spectral holes (PIRSHs) have been generated in the electronic ground state inside the inhomogeneously broadened vibrational absorption bands of various molecule:chalcogenide glass combinations. They all show persistent IR spectral holes and spontaneous hole filling at low temperatures. A remarkable result is that the quantitative form of the nonexponential hole relaxation depends solely on the average coordination number of the glass independent of chemical composition.

(b) PIRSH Burning of Tb^{3+} in Alkaline Earth Fluoride Crystals: Surprisingly these PIRSHs in "glassy" crystals display the characteristic properties of spectral holes burned in true glasses, including highly non-exponential hole relaxation on time scales ranging from a few minutes to many hours, and a broad distribution of barriers observable in thermal cycling studies.

(c) NO_2^- Ions in Alkali Halides: Four different kinds of vibrational hole burning for various NO_2^-:host combinations have been carried out. They are: (1) the hole and antihole in the same absorption line, (2) the antihole removed in frequency from the inhomogeneously broadened line, (3) multiple antiholes and (4) the burning at one vibrational mode frequency while monitoring the persistent changes produced in the other internal (IR) or external (FIR) modes with a high resolution FT interferometer.

(d) Calculations and Simulations of Stationary Vibrational Solitons in Crystals: In some ways the stationary localized mode results for perfect anharmonic crystals are reminiscent of the defect induced local modes studied in the harmonic approximation. For example, a monatomic 1-D lattice produces a vibrational soliton above the plane wave spectrum and a diatomic one gives intrinsic vibrational solitons both in the gap between the optic and acoustic plane wave spectrum as well as above the optic branch.

(e) $KI:Ag^+$ Vibrational Dynamics: First Evidence for Vibrational Solitons: The silver ion in KI is the most thermally unstable lattice-defect combination known. Why? It now appears that the occurrence of rapid temperature dependences in defect signatures such as the optical properties of "harmonic-like" vibrational modes observed in KI:Ag+ at low temperatures may result from localized anharmonic modes being released into the lattice.

II. PROGRESS

Persistent spectral hole burning (PSHB) is a high-resolution laser spectroscopic technique which provides a means of probing the microscopic dynamics of a solid through its interactions with optically active impurity molecules. In essence, the technique uses a narrow bandwidth laser to selectively bleach the optical absorption arising from the small subset of impurities which happen to be in resonance with the laser frequency. The resulting reduction in absorption strength in the narrow frequency region about the laser frequency is known as a "spectral hole" and if the lifetime of this hole is longer than any of the impurity excited state lifetimes, the hole is said to be persistent. Persistent hole lifetimes at liquid helium temperatures typically range from a few seconds to many hours or even days. The utility of the phenomenon lies in the fact that, because only those centers in resonance with the laser are involved in the hole burning, it is possible to extract the lifetime-limited homogeneous linewidth, which would ordinarily be obscured within the disorder-dominated inhomogeneous absorption band. Furthermore, because in glasses the hole burning process itself is intimately connected with the existence of multiple metastable configurations of the glass, it is possible, by studying the time evolution of the spectral hole, to learn about the low temperature relaxation dynamics among these glassy configurations.

Persistent spectral hole burning is to be contrasted with the older technique of transient saturation hole burning.[1,2] The latter is a high intensity technique, requiring that the rate at which photons are absorbed be comparable to the rate at which the impurities relax back to their ground state; intensities used are typically several kW/cm^2, and these holes persist only as long as the excited state lifetime, typically on the order of a nanosecond. In persistent spectral hole burning, high laser intensities are not required. The long lifetime of the effect makes it possible for a spectral hole to gradually build up over time, even at low intensity.

A number of high resolution laser experiments have been carried out at Cornell over the past three years which demonstrate that persistent IR spectral holes (PIRSHs) can be generated at low temperatures in the vibrational spectrum of small molecules, matrix isolated in crystals[3] and glasses[4-6] even though no electronic excitation is involved, i.e., non-photochemical processes. Commercial low power single mode Pb-salt diode lasers (~10 to 100 μW) have provided a near ideal cw source for generating persistent IR spectral holes (PIRSHs) at low temperatures in solids. The holes can be produced and probed with a single laser, focused to an intensity at the sample typically up to 100 mW/cm^2. The union of the IR Pb-salt diode laser and broad band FT interferometric methods has produced a new high resolution spectroscopic technique for investigating both the statics and dynamics of these molecules. In the discussion below we describe in more detail how this probe has been used to learn about a variety of solid state dynamical processes.

A. Hole Burning in Chalcogenide Glasses

1. Introduction

The discovery of PIRSH burning for the sulfur-hydrogen stretch mode in hydrogenated As_2S_3 glass demonstrated for the first time that vibrational hole burning was not restricted to ionic and Van der Waals solids, but could occur in covalently bonded glasses as well.[4,5] It was soon found[6] that the As_2S_3:SH system was not an anomaly, but rather the first in a broad class of systems. Several new host-impurity combinations, including D_2O, OD, and CO_2 in As_2S_3, SeH and CO_2 in glassy Se, and SeH in As_2Se_3, have been successfully prepared, and all exhibit PIRSH burning. So far, PIRSH burning appears to be a universal phenomenon in the chalcogenides.

A number of factors make impurity vibrational modes particularly well-suited for persistent hole burning studies of the chalcogenides. The first of these is the matter of finding an impurity which absorbs at a frequency where the host is transparent. Since persistent hole burning typically relies on absorptions due to dilute impurities, relatively thick samples, on the order of a few millimeters, are usually required to obtain the necessary absorption strength. It is thus imperative that the experiments be performed in a frequency region in which the host is transparent. The infrared-active vibrational modes of molecules made up of relatively light atoms have frequencies which fall nicely within the transparent window of the chalcogenides, between the bulk phonon absorption and the electronic band gap.

A second consideration is the ease with which the impurity can be introduced into the host. An impurity with absorption at the right frequency is, after all, of no use if it is insoluble in the host material. In this respect, the small, light molecules used here again appear to be ideal. It was recognized as early as 1953 that exposing molten chalcogenides to air could lead to new IR absorptions in the melt-quenched glass, although at that time the species present in the glass were not identified.[7] Thus common atmospheric gases were obvious candidates for producing hole burning defects. It has been found that many of these molecules, such as CO_2 and water, go into chalcogenide glasses so easily, and exist in the atmosphere in such large concentrations, that it is very difficult to produce a sample *without* these impurities. Since chalcogenide glasses are emerging as important materials for IR optical fiber applications, a better understanding of these common defects is desirable.

Finally , because the chalcogenides are good glass formers over such a wide range of alloy compositions, they offer a promising system for attacking the general problem of persistent hole burning in glasses. The discovery of PIRSH burning in this system presents the possibility of systematically determining correlations between the hole burning behavior and other composition-determined properties of the glass. This work is still in its very early stages, but it will be seen that substantial variations in hole burning behavior do exist within the chalcogenide system.

Glasses of As_2S_3, Se, As_2Se_3 as well as the alloy Ge-As-Se have all been doped with small molecules and examined by PIRSH burning. We find that all molecule:glass combinations show PIRSH burning and spontaneous hole filling at low temperatures. A diverse set of impurities in a single host display very similar relaxation behavior, while identical impurities in different hosts show strikingly different behavior. These results demonstrate the dominant role of the host in determining the hole relaxation behavior. A similar pattern emerges for the hole widths in the various systems in that the temperature dependence of the width appears to be determined solely by the host, independent of the defect involved.

2. Discussion of the Findings

Examination of the infrared spectra allows unambiguous identification of the impurities introduced in the doping process, and provides some information on the interactions between the host and impurity. Key features of the infrared spectra are summarized in Table 1.

Table 1. IR absorption band positions, inhomogeneous widths and hole widths at 1.5 K for vibrational modes of various impurities in chalcogenide glasses.

Host	Impurity	Peak Frequency (cm^{-1})	Width (FWHM) (cm^{-1})	Hole Width (FWHM) at 1.5K (GHz)
As_2S_3	$^{12}C^{16}O_2$	2323.2	6	0.080 ± 0.003
	$^{13}C^{16}O_2$	2258.0	6	—
	$^{18}O^{12}C^{16}O$	2306.5	6	—
a-Se	$^{12}C^{16}O_2$	2321.0	6	0.080 ± 0.005
		641	~ 20	—
As_2S_3	SH	2485	74	0.8 – 15 *
	SD	1807	51	0.6 *
a-Se	SeH	2194	53	0.81 – 8.5 *
	SeD	1589	33	—
As_2Se_3	SeH	2189	108	1.1 – 10 *
As_2S_3	D_2O	2679	59	1
		1170	19	—
	OD	2566	95	1

*Depends on burn frequency. Range indicated is merely that observed to date; actual upper limit is probably much greater.

a. Temperature dependence of the hole width

Despite the considerable differences in the homogeneous and inhomogeneous widths for CO_2 and SH in As_2S_3 shown in Table 1, and the strong burn frequency dependence of the hole width observed for the latter, the temperature dependences of the hole width of these two defects in this host are remarkably similar. Figure 1 shows the hole width as a function of temperature for the SH defect in As_2S_3 for two burn frequencies, open circles and triangles. The temperature

dependence of the hole width for CO_2 in As_2S_3 is shown by the open squares in Fig. 1(b). The insert presents a low temperature and high temperature hole burnt spectrum. In all cases the hole is burned and probed at the same temperature.

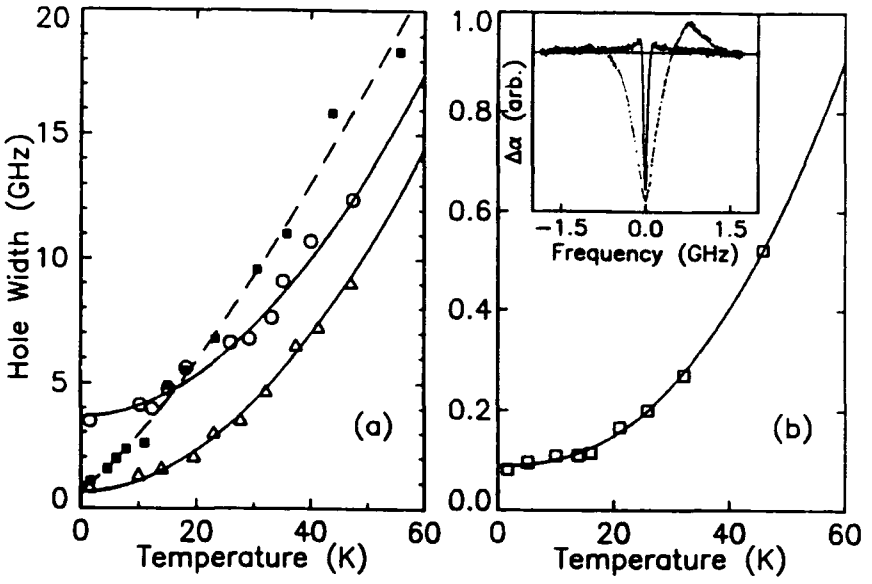

Figure 1. Hole width (FWHM) as a function of temperature. In each case, holes are burned and probed at the same temperature. Lines are power law fits described in text. (a) SeH in *a*-Se burned at 2209 cm^{-1} (solid squares, dashed line), and SH in As_2S_3 burned at 2504 cm^{-1} (open triangles) and at 2463 cm^{-1} (open circles). (b) CO_2 in As_2S_3 burned at 2324.2 cm^{-1}. Inset shows the appearance of the hole at 1.6 K (narrow hole) and at 46 K. Plotted is the laser-induced change in absorption versus the offset from the burning frequency. The vertical scale for the much shallower 46 K hole has been expanded to allow comparison of shapes.

In each case note that the hole width does not appear to vanish as T approaches zero, but rather approaches a finite value not significantly smaller than the width at 1.5 K. Above this low temperature value, which is presumably determined by the excited state lifetime, the hole width increases approximately as T^2.for the open circles, triangles and squares. The hole width $\Delta\nu$ (T) is well described, over the entire temperature range studied, by a power law of the form

$$\Delta\nu\,(T) = \Delta\nu_0 + a\,T^b. \qquad (1)$$

The best fit for CO_2 in As_2S_3 is obtained with $\Delta\nu_0 = 80$ MHz, the temperature exponent $b = (2.2 \pm 0.3)$, and $a = 0.096$ MHz / $K^{2.2}$, as shown by the solid line in Fig. 1(b). Fits to the two data sets for the SH defect in As_2S_3 yield the following values: temperature exponent $b = (1.97 \pm .1)$, and the coefficient $a = 3.4 \times 10^{-3}$ GHz/ $K^{1.97}$. The zero temperature widths are $\Delta\nu_0 = 0.8$ GHz and $\Delta\nu_0 = 3.6$ GHz for the 2503 cm^{-1} and 2462 cm^{-1} data, respectively. Note that for the two

burn frequencies shown for the SH defect, only $\Delta\nu_0$ differs, while a and b are apparently independent of the burn frequency.

Though the temperature dependences for two different defects in As_2S_3 are virtually identical, the behavior in a different host, *a*-Se, shows obvious differences. The solid squares in Fig. 1(a) represent the hole width as a function of temperature for the SeH defect in *a*-Se between 1.6 K and 56 K for holes burned at 2209 cm^{-1}. For comparison, the 2503 cm^{-1} data for SH in As_2S_3 are also included. The *a*-Se:SeH data can again be fit over the entire temperature range using Eq. 1, but the hole width no longer goes as T^2. Instead the fit yields temperature exponent b = (1.27 ± 0.1), with $\Delta\nu_0$ = 0.79 GHz, and a = 0.11 GHz/ $K^{1.27}$. It is clear that, although the hole width for *a*–Se:SeH increases more rapidly with temperature than does that for As_2S_3:SH, it does so in a more nearly linear fashion.

The problem of optical dephasing in glasses has drawn much attention[8] ever since it was first discovered[9,10] that homogeneous linewidths for rare earth ions in inorganic glasses at low temperatures are much larger and follow very different temperature dependences than those for the same impurities in crystalline hosts. The experimental picture has become more complex with the temperature dependence below 10 K varying from $T^{1.0}$ to $T^{2.2}$ for a wide range of impurities in both organic and inorganic systems, with little apparent pattern to these results, except possibly for the rough tendency for organic systems to fall neat $T^{1.3}$ and for inorganic systems to fall near T^2. A variety of theoretical models have been put forward to account for these properties.[11-14]

The obvious difference between the two glasses examined here is that Se glass consists of weakly interacting chains of two-fold coordinated Se atoms, while in As_2Se_3 these chains are cross-linked by three-fold coordinated As atoms. This result suggests a relation between the microscopic topology of the glass network and hole relaxation behavior, but chemical effects due to the presence or absence of As can not be ruled out. The importance of this result, however, is that both glasses are members of a large class of glass-forming alloys which allow continuous variation of structure by varying alloy composition, opening the way for a systematic study of the effects of network topology on spectral hole behavior.

The role of microscopic topology in determining the properties of glass-forming compounds has been explored theoretically for several years. The concept of an average atomic coordination number was used by Phillips[15] in constraint counting arguments explaining the strong glass-forming tendency of certain alloy compositions. These ideas were later refined by Thorpe et al.[16–18] who, by evaluating the number of zero-frequency "floppy" modes as a function of the coordination number, predicted a rigidity percolation transition from a soft to a rigid structure should occur at a coordination number of 2.4.

The ternary Ge–As–Se system is particularly well-suited to testing the validity of these

topological concepts because its large glass-forming region makes it possible for a given value of the average coordination number <r> (given in this case by $<r> = 4X_{Ge}+3X_{As}+2X_{Se}$, where X is the mole fraction) to be realized with a continuous range of chemical compositions, allowing purely topological effects to be distinguished from chemical effects.

b. Spontaneous hole filling in the ternary Ge–As–Se system.

After burning ceases, PIRSHs burned in all these glass systems are observed to decay in a strongly non-exponential manner. One aspect of the PIRSH burning behavior of molecular impurities in chalcogenide glasses which sets these systems apart is that the spontaneous relaxation from the burned to unburned configurations takes place on an experimentally accessible time scale, allowing this relaxation to be observed over a much wider dynamic range than in the much more slowly relaxing amorphous systems studied in the visible by other workers.[19,20]

Infrared absorption spectra showing the SeH stretch absorption bands produced in the various host alloy glasses by this procedure are displayed in Fig. 2. Note that the SeH bands, all having maxima at roughly 2200 cm^{-1} and widths on the order of 50 cm^{-1}, have considerable frequency overlap among the various hosts, allowing hole burning experiments to be carried out at a single frequency in all samples.

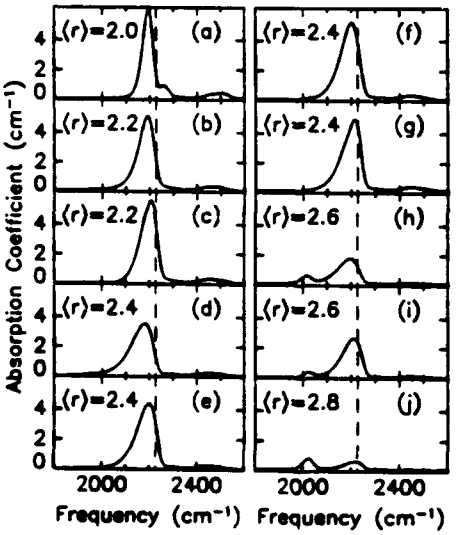

Figure 2. Infrared absorption spectra at 1.5 K, showing the SeH stretch bands in ten glasses in the Ge–As–Se system: (a) glassy Se, (b) $As_{0.2}Se_{0.8}$, (c) $Ge_{0.089}As_{0.022}Se_{0.889}$, (d) As_2Se_3, (e) $Ge_{0.1}As_{0.2}Se_{0.7}$, (f) $Ge_{0.133}As_{0.133}Se_{0.733}$, (g) $Ge_{0.15}As_{0.10}Se_{0.75}$, (h), $Ge_{0.1}As_{0.4}Se_{0.5}$, (i) $Ge_{0.2}As_{0.2}Se_{0.6}$, and (j) $Ge_{0.3}As_{0.2}Se_{0.5}$. The value of the average coordination number <r> is noted for each spectrum. The vertical line indicates the laser frequency 2227 cm^{-1}, used in the hole burning experiments.

Figure 3 displays the results of the 1.5 K hole relaxation experiment for ten compositions in the Ge–As–Se system, chosen so that there are two compositions having <r> = 2.2, four having <r> = 2.4, two having <r> =2.6, and one composition each for <r> =2.0 and <r> = 2.8 The hole depth, plotted as a function of the time t after burning ceases, is normalized to unity at t=0 for each composition.

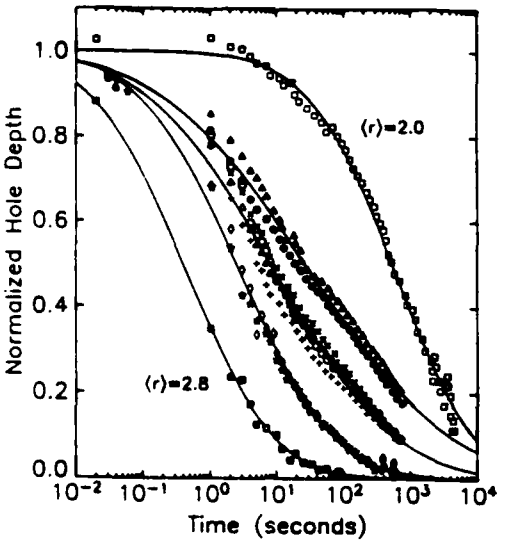

Figure 3. Spectral hole refilling at 1.5 K for the SeH absorption in Ge–As–Se glasses. Data points show the hole depth, normalized to unity at t=0, as a function of time t after burning ceases for ten different compositions burned and probed under identical conditions. The average atomic coordination numbers <r> and compositions of the ten samples, listed in order of decreasing relaxation time, are as follows: <r> = 2.0 — glassy Se (open squares); <r> = 2.2 — $As_{0.2}Se_{0.8}$ (solid triangles), $Ge_{0.089}As_{0.022}Se_{0.889}$ (solid circles); <r> = 2.4 — $Ge_{0.15}As_{0.10}Se_{0.75}$ (0); As_2Se_3 (open circles), $Ge_{0.1}As_{0.2}Se_{0.7}$ (open triangles), $Ge_{0.133}As_{0.133}Se_{0.733}$ (+), <r> = 2.6 — $Ge_{0.1}As_{0.4}Se_{0.5}$ (open diamonds), $Ge_{0.2}As_{0.2}Se_{0.6}$ (open stars); <r> = 2.8 — $Ge_{0.3}As_{0.2}Se_{0.5}$ (solid squares). Solid lines are fits, for each set of compositions having a given value of <r>, to a Gaussian distribution of tunneling parameters, described in the text.

The key result is that all compositions having a given value of <r> follow virtually identical hole relaxation curves. Throughout the composition range studied here, the overall hole relaxation rate increases monotonically with <r>, with holes at <r>=2.8 decaying over three orders of magnitude faster than those at <r>=2.0. This monotonic variation with <r>, however, shows no indication of a rigidity transition or any other unusual features at <r> = 2.4.

The direction of the trend exhibited in the present results, slow relaxation at small <r> and rapid relaxation at large <r>, is quite surprising if one takes the simplistic view that refilling rates

are determined primarily by the height of the barriers between configurations, and that large barriers correspond to a more rigid structure. Such a view would predict that since systems with small values of <r> have the least rigid structures, relaxation would be most rapid in these systems, the opposite of the observed trend. Clearly a more sophisticated approach of enumerating as a function of <r> the configurations available to hole burning and the barriers between them is required to explain these results.

Given the complexity of glassy systems, however, the existence of a single simple parameter, <r>, which can predict spectral hole relaxation behavior is remarkable indeed. The implication, that simple geometrical considerations play the predominant role in determining spectral hole burning behavior, should prove an invaluable clue in the quest for a microscopic theoretical understanding of low temperature relaxation phenomena in glasses.[21]

B. Persistent IR Spectral Hole Burning of Tb^{3+} in Alkaline Earth Fluoride Crystals

1. Introduction

Persistent non-photochemical spectral hole burning, in which an electronic state is excited but the defect returns to the initial electronic configuration during the hole burning process, has been observed for a wide variety of impurities in glasses.[19,20] The standard model for non-photochemical hole burning in glasses[19] assumes that excitation of the impurity leads to a configuration change in the host surrounding the impurity, resulting in a shift of the impurity transition frequency away from the frequency of the exciting laser. The large number of nearly degenerate configurations available to the atoms of the glass, prerequisite for hole burning by this mechanism, is also invoked in the tunneling model[22,23] for the low temperature thermal properties of glasses. The observation[24] of glass-like low temperature specific heat, thermal conductivity and internal friction in the mixed crystal $Ba_{1-x}La_xF_{2+x}$ suggests that this class of materials, like glasses, may have the multiple configurations necessary for non-photochemical hole burning. But will an inner shell f state IR transition provide enough of a kick to the surroundings to disturb the local environment around the rare earth ion?

This past year we have found persistent IR spectral holes in the inhomogeneously broadened 4.5 μm $^7F_6$ –> $^7F_5$ electronic absorption band of the Tb^{3+} ion in the mixed crystal $Ba_{1-x-y}La_xTb_yF_{2+x+y}$. These PIRSHs display the characteristic properties of spectral holes burned in true glasses, including highly non-exponential hole relaxation on time scales ranging from a few minutes to many hours, and a broad distribution of barriers observable in thermal cycling studies.[25]

2. Results and Discussion

Like La, Tb forms a 3+ ion when introduced into BaF_2, and substitution of either La^{3+} or

Tb^{3+} for Ba^{2+} results in a nearby interstitial F^- ion necessary for charge neutrality. Similar glasslike behavior is therefore expected to be produced by the introduction of either La^{3+} or Tb^{3+} ions; however, the unfilled f shell of Tb^{3+} produces absorption lines in the IR.

Infrared absorption spectra at 1.6 K for samples having various La and Tb concentrations are shown in Fig. 4. The overall effect of increasing the lanthanide concentration is to increase the degree of inhomogeneous broadening of the Tb^{3+} electronic transitions, so that sharp lines associated with a specific defect cluster apparent at relatively low concentrations eventually broaden and merge into a single inhomogeneous band at the highest concentrations.

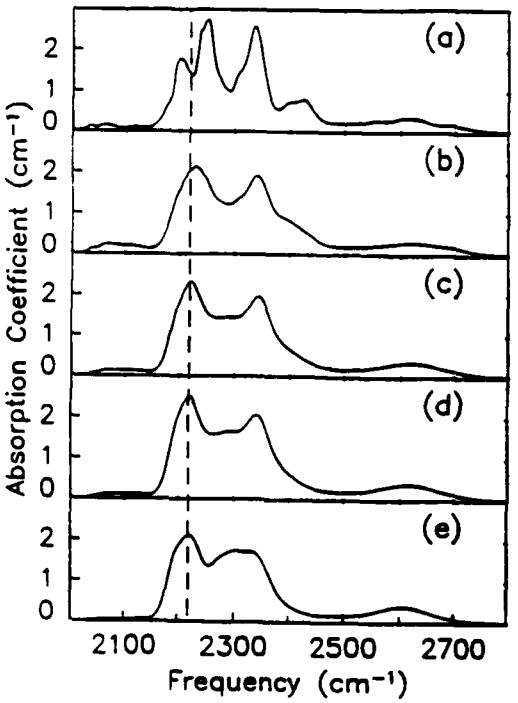

Figure 4. Infrared absorption spectra of $Ba_{1-x-y}La_xTb_yF_{2+x+y}$ mixed crystals at 1.6 K, showing the Tb3+ f-shell electronic transitions. The La and Tb fractions, x and y, are (a) x = 0, y = 0.05, (b) x = 0.05, y = 0.05, (c) x = 0.10, y = 0.05, (d) x = 0.15, y = 0.05, (b) x = 0.30, y = 0.05. The vertical line indicates the laser frequency, 2220.2 cm^{-1}, used in determining the hole burning quantum efficiency for each composition.

PIRSH burning has been observed for $Ba_{1-x-y}La_xTb_yF_{2+x+y}$ samples having the following four compositions: y = 0.05; x = 0.05, 0.10, 0.15, and 0.3.

A possible mechanism for spectral hole burning which we have been able to rule out is an internal relaxation bottleneck in the Tb^{3+} ion itself. We have observed hole burning by such an internal optical pumping mechanism in another rare-earth-doped alkaline earth system, $CaF_2:Pr^{3+}$.

In this system we observe spectral hole burning for transitions in the crystal field split $^3H_4 \rightarrow {}^3H_5$ manifold at roughly 4.5 μm. Our results are that for 1.0 atomic percent Pr^{3+}, the transition at 2182 cm^{-1} produces a complicated spectrum of holes and antiholes with the antihole falling at the laser frequency. All of these holes relax exponentially at 1.6 K with a lifetime of 36 ± 1 s. This behavior is reminiscent of that observed for Pr^{3+} hole burning in the visible region, for which the hole burning mechanism is optically pumped population redistribution among the hyperfine-[26] or superhyperfine-split[27] ground levels of the Pr^{3+} ion, with hole filling occurring at the characteristic spin-lattice relaxation rate.[28] The present results for CaF_2: Pr^{3+} $^3H_4 \rightarrow {}^3H_5$ transitions are the first instances of hole burning by this optical pumping mechanism to be observed in the mid-infrared region.

To test whether PIRSH burning in the $Ba_{1-x-y}La_xTb_yF_{2+x+y}$ system could be due to such a mechanism, we investigated a sample with no La and only 0.5 percent Tb. Since hole burning via internal population redistribution of the ion itself should occur at any concentration this low concentration sample would display PIRSH burning similar to the other samples if the optical pumping scheme were responsible. Since no effect was seen we have been able to rule out the internal optical pumping mechanism for the $Ba_{1-x-y}La_xTb_yF_{2+x+y}$ system. That the hole burning mechanism in is not internal optical pumping is further emphasized by the highly non-exponential nature of the hole decay, with very long hole lifetimes (many hours) occurring at the slow end of the distribution of relaxation rates.

With PIRSH burning we have identified two unusual properties of the $Ba_{1-x-y}La_xTb_yF_{2+x+y}$ system. One is that the hole burning quantum efficiency is independent of the La concentration. One might have expected a dramatic increase in the quantum efficiency on the grounds that increasing La^{3+} would increase the fraction of Tb^{3+} sites having sufficient local configurational multiplicity for hole burning. The results however suggest that the effect is already nearly saturated by the presence of Tb^{3+} itself at concentration of 5 %. This is consistent with the idea that that the multiple configurations associated with hole burning are somehow associated with the F^- interstitials which are produced by the introduction of trivalent rare earth ions. The absence of hole burning for the low concentration sample implies that hole burning only occurs when the trivalent impurity concentration, and hence the density of interstitials, is greater than some critical value, somewhere between 0.5 and 5%.

The other unusual property has to do with PIRSH relaxation. Monitoring the evolution of the hole size after burning ceases reveals highly non-exponential refilling following a form virtually identical to that observed for PIRSHs burned in glasses as described in the previous section. Figure 5 shows the integrated area of the PIRSH burned and probed at 1.6 K, proportional to the number of centers remaining in the hole burned configuration, plotted as a function of time after the burning laser is removed, for two compositions, (x = y = 0.05), and (x = 0.30, y = 0.05). The

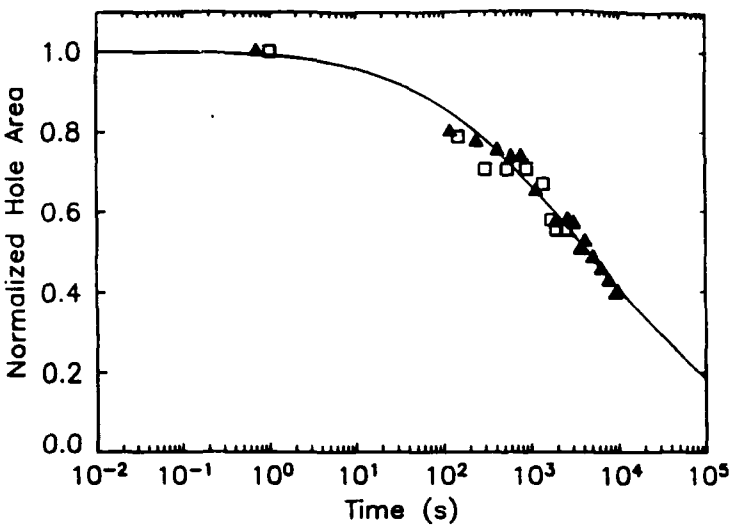

Figure 5. PIRSH relaxation at 1.6 K for two compositions in the $Ba_{1-x-y}La_xTb_yF_{2+x+y}$ system, x = 0.05, y = 0.05 (solid triangles) and x = 0.05, y = 0.30 (open squares). Plotted for each case is the integrated area of the spectral hole as a function of time after burning ceases, with the hole area normalized to unity at t = 0. The initial holes were burned for 15 minutes at 2220 cm^{-1},. Solid line is a fit to a gaussian distribution of tunneling parameters.

PIRSH relaxation behavior for the two compositions is identical within experimental error.

The important conclusion is that persistent spectral holes have been observed for the first time for a non-photochemical transition of a rare earth ion in a crystal. The results are strikingly similar to non-photochemical hole burning in glasses. See for example, Fig. 3. Both the highly nonexponential hole relaxation at 1.6 K and the broad distribution of barrier heights seen in thermal hole erasure measurements are typical signatures for glassy systems. It is quite surprising that the frequency independent density of tunneling states found in glasses to produce persistent hole burning can be generated in a single crystal with a localized electronic defect plus a vacancy.

C. NO_2^- Ions in Alkali Halides

1. Hole Burning on the Internal Bending Vibrational Mode of NO_2^-

Glassy behavior in crystals needs to be characterized more completely. One way to do this is to return to the simplest possible crystal and identify what are the minimum conditions for the persistent spectra effects. In our attempt to enumerate the different possibilities we have found that vibrational manifold burning generates multiple persistent effects.

The asymmetrical bending mode transition of NO_2^- in KCl and KBr consists of a complex spectrum made up of five absorption lines, four components symmetrically spaced around a weak central line.[29] Hole burning at any of the four components produces additional satellite holes in the other three, indicating that all four lines stem from the same dynamical properties of an

individual molecule. A typical spectrum is presented in Fig. 6.

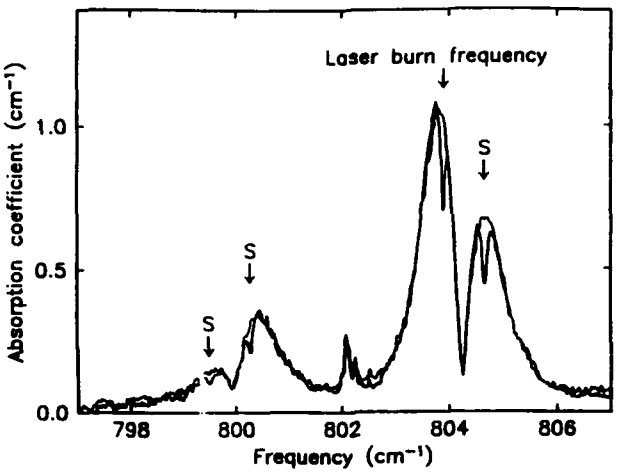

Figure 6. Manifold IR hole burning in the bending mode absorption spectrum of KCl + 0.012% KNO_2 at 1.6 K. Two interferometer traces are shown at 0.03 cm^{-1} resolution, one before and one after a hole is burned with a diode laser at a frequency of 803.91 cm^{-1}. The burned spectrum contains not only the sharp hole at this frequency but also three other satellite holes labeled (S).

Such experiments have shown that the complex spectrum is produced by rotational tunneling of the N about the O-O axis, which is fixed in the octahedral cage, and that the hole burning is associated with the reorientation of the O-O axis in the crystal. Hence the bending mode spectrum can be described by a Q branch surrounded by P and R branches.

Another persistent effect that we have uncovered for this lattice-defect system consists of burning at one vibrational mode frequency while monitoring the persistent changes produced in the other internal or external (localized phonon) modes with a high resolution FT interferometer. This procedure has been used effectively to identify the localized phonon modes of the particular defect-lattice system.[30,31] When NO_2^- is doped into KI, a single bending mode transition results, different from that previously described for KCl and KBr hosts. PIRSH burning on this transition confirms that the equilibrium molecular orientation, has the permanent dipole along the <100> direction with the molecule plane in a <110> direction which is not the same as for the other two hosts.

In addition to the internal vibrational modes of the molecule, three low lying far IR excitations are found at frequencies in the gap between the optic and acoustic phonon branches. By doping the crystal with molecules containing an isotopic mixture of N-14 and 15, as well as O-16 and 18, and then monitoring the forest of far IR lines in the KI gap region while sequentially burning on each of the isotope-shifted IR bending modes with the diode laser, the far IR isotope shifts of all of the gap-mode isotopic combinations have been identified. See Fig. 7. The different

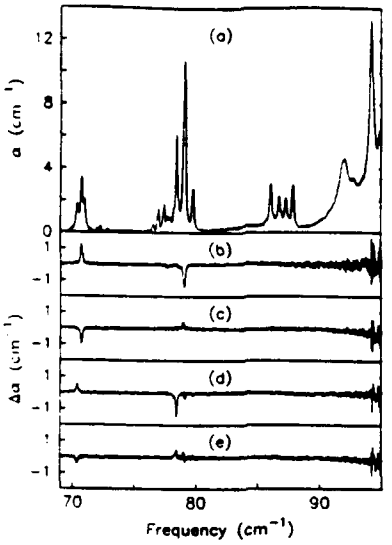

Figure 7. Spectral changes in the FIR gap modes produced by hole burning the isotope shifted IR bending mode of NO_2^-. (a) The FIR spectrum of KI nominally doped with 0.1% KNO_3 (40% ^{18}O enrichment). (b) and (c) show the FIR gap mode absorption changes produced by burning the (14,16,18) IR ν_2 mode with laser polarization parallel and perpendicular to the interferometer beam axis. (d) and (e) are the gap mode changes produced by burning the (14,18,18) IR ν_2 mode with the same two laser polarizations.

far IR isotope shifts for the different lines show for the first time that the lowest and highest frequency transitions in the gap are due to translational localized modes of the NO_2^- defect, while the third has a mixed translational-librational character.[31] Such information is crucial for any lattice dynamical calculation of this low symmetry defect-lattice system. The general conclusion is that vibrational hole burning can be expected to influence the entire spectrum produced by the defect, including the impurity induced absorption in the phonon spectrum. No glassy states are associated with the persistence observed in this system.

D. Calculations and Simulations of Stationary Vibrational Solitons in Crystals.

1. Procedure

The possibility of intrinsic localized modes in pure anharmonic crystals for sufficiently strong quartic anharmonicity[32-34] has been confirmed by numerical simulation studies[35,36] in one and two dimensions. In some ways the results are reminiscent of the defect induced local modes. For example, the one simulation for a 1-D diatomic anharmonic lattice shows that intrinsic local modes appear both in the gap between the optic and acoustic plane wave spectrum as well as above the optic branch[36] similar to the spectrum generated by a point defect in a harmonic diatomic lattice.[37] Although the original analytical study[32] focused on the odd parity vibrational mode, which in one dimension has essentially the amplitude pattern of a simple triatomic molecule, both

the simulations[35,36] and the more recent analytical work by Page[38] have shown that an unusual even parity mode with the vibrational pattern of a diatomic molecule also exists. So far all efforts have been directed at characterizing and understanding the large anharmonicity regime.

We have studied analytically an experimentally relevant problem: the influence of hard but small quartic anharmonicity on the vibrational spectrum of a monatomic lattice with nearest neighbor force constants.[39] We find that both odd and even localized modes are possible for all values of the anharmonicity parameter but the odd mode is determined to be the fundamental intrinsic localized excitation. With a first order correction to the rotating wave approximation we also demonstrate that the frequency of the odd mode at ω_L as a function of the anharmonicity parameter is red-shifted by a few percent due to the presence of a higher frequency local mode at $3\omega_L$. In all cases the amplitude at $3\omega_L$ is a small fraction of the amplitude at ω_L so that the response from still higher frequency components at $5\omega_L$, etc., can be ignored. Typical results obtained from these calculations are shown in Fig. 8.

For weak anharmonicity these modes become delocalized, while they take on the vibrational pattern of a small molecule when the anharmonicity becomes large. This identification of the weak anharmonicity limit permits us for the first time to address the question of the existence of anharmonic local modes in ideal crystals. With anharmonic parameters similar to those found in alkali halide crystals the energy needed to produce these modes in all three dimensions is estimated. We find that thermal motion alone may not provide enough amplitude to support these modes in a

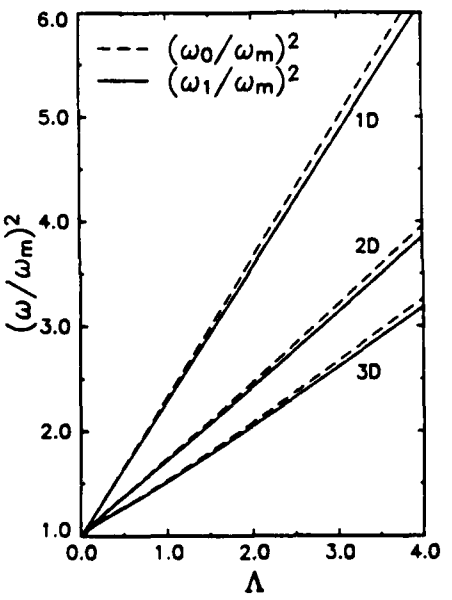

Figure 8. Local mode frequency versus Λ as calculated by two different rotating wave approximations. The dashed curve follows from the single frequency rotating wave approximation while the solid curve includes an additional contribution from the third harmonic term.

lattice with the anharmonicity of pure LiF. On the other hand, at some defect sites the requirements could be less severe and anharmonic modes might be generated by a nonthermal process such as an optical excitation of the F center, which introduces an energy equivalent of ~40 Debye phonons into the lattice. The large anharmonicities found in solid He and near ferroelectric systems should provide friendly environments for these localized modes.

For the particular case of a 2-D square lattice the simulations for a number of different initial conditions have been made into a video. We have found that the difficulty associated with interpreting the dynamics of the coupled nonlinear equations is completely bypassed when the video is viewed first. The set of force equations to be studied have the form

$$m\frac{d^2u_n}{dt^2} = K_2(u_{n+1} + u_{n-1} - 2u_n) + K_4[(u_{n+1} - u_n)^3 - (u_n - u_{n-1})^3], \qquad (2)$$

where K_2 is the harmonic and K_4 the anharmonic force constant, a is the magnitude of the magnitude particle displacement and the relative strength of the anharmonicity is given in terms of the dimensionless parameter $\Lambda = K_4\alpha^2/K_2$. For sufficiently large Λ a local mode appears above the top of the plane wave spectrum for the anharmonic lattice.

This effect is illustrated in a number of ways. First by showing the dynamics for a harmonic lattice and an anharmonic lattice excited at the same time with the initial condition shown at the top left of Fig. (9) For the harmonic lattice the excitation rapidly moves away from the point of excitation until all particles have the same amplitude. Since the lattice has 20 x 20 particles, this amplitude is imperceptible on the TV screen. In contrast the anharmonic lattice picture displays a localized excitation throughout the viewing interval. The next scene, using the same initial conditions, compares a large amplitude displacement with a small amplitude one both for the anharmonic lattice. Since the small amplitude was chosen such that a local mode would not be formed the time evolution of this picture looks the same as for the harmonic lattice, i.e., the excitation spreads evenly over the entire array of particles.

The rest of the scenes show the interesting results that can be generated by superposition. If two odd modes are started on next neighbor sites with amplitudes of their respective eigenvectors π out of phase with each other as shown at the top right of Fig. (9) then the result is a vibrating even mode. Next four odd modes are superimposed on the four next neighbor sites, again π out of phase with each other as shown at the lower right of Fig. (9). The result is a breathing vibrational mode, as long as the transverse and longitudinal force constant are set equal to each other. If the transverse force constant are less than 0.9 of the longitudinal, we find that the breathing mode breaks up into four separate modes which are repelled from each other and move out along the $\pm$ x

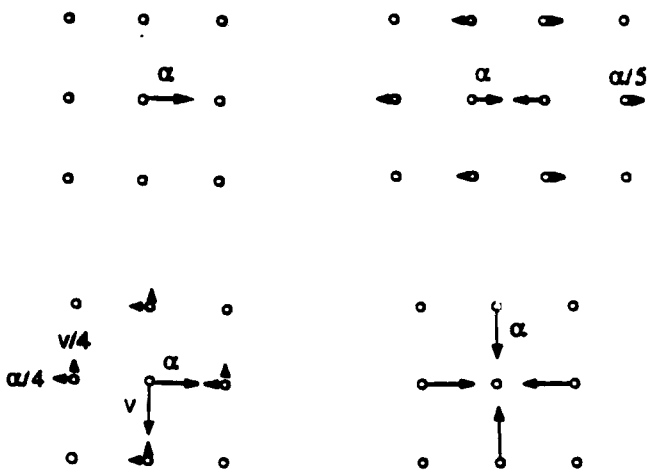

Figure 9. Initial conditions for a two dimensional square lattice to illustrate different simulation results. In the top left frame a single particle is plucked with amplitude α at t = 0 and subsequently the amplitude of all atoms are determined as a function of time. The top right frame shows the superposition of two odd modes on neighboring lattice sites. The lower right frame shows the initial conditions for four odd modes on next nearest neighbor sites. The lower left frame shows the circularly polarized initial condition with maximum amplitude in the x direction and maximum velocity in the y direction for an odd mode.

and y axes. Finally we have investigated an odd mode with maximum amplitude in the x direction and maximum velocity in the y direction at t = 0 as shown at the bottom left of Fig. (9). The result is a circularly polarized localized vibrational mode which carries angular momentum. The most surprising thing about each of these superposition examples is that it works. Recall that the localized modes are solutions of coupled nonlinear equations.

E. KI:Ag^+ Vibrational Dynamics: First Evidence for Vibrational Solitons in Crystals

1. Introduction

The silver ion in KI is the most thermally unstable lattice-defect combination known. At 1.2 K the Ag^+ ion takes the same equilibrium position as the K^+ ion it replaces but by 20 K it is in an off-center position.[40,41] A fundamental problem is to understand within the framework of lattice dynamics how the system can move so rapidly between these two lattice-defect arrangements with temperature.

To experimentally track the temperature dependence of different aspects of the coupled defect-host system, we have made UV measurements which follow the Ag^+ ion itself and then

Raman scattering results which monitor the disappearance of the E_g mode and the appearance of a new A_1 symmetry resonant mode as the temperature is raised. Page has calculated the spectral properties of IR and Raman active features for the on-center configuration and finds that the harmonic approximation gives a good account of the low temperature IR and Raman data, for a model in which the defect and surrounding host ions remain strongly coupled yet are quite close to being unstable against T_{1u} displacements. The results together imply that the observed temperature dependence of the on-center spectral features simply reflects the population in this state. The system is in either the ground state configuration or not; a continuous evolution of the on-center defect dynamics with temperature does not occur.

2. Results

To monitor the position of the Ag^+ ion with temperature we make use of the known optical behavior of this ion in alkali halide crystals, which can be understood in terms of the $4d^{10} \rightarrow 4d^9 5s$ parity forbidden transitions of the defect.[42] These transitions are made allowed by vibronic coupling to the odd parity vibrational modes, or if the defect is off center, by the static odd parity lattice displacement; the larger the odd parity contribution the larger the line strength.

Figure (10a) shows the measured UV absorption spectrum of KI:Ag^+ for two different temperatures. Note that over this temperature range the center frequencies remain essentially fixed. A linear concentration dependence establishes that these three features, labeled A, A' and C in the nomenclature of Ref.43, are associated with isolated Ag^+ ions. To display the three lines in one figure, three different Ag^+ concentrations are required as described in the caption. The strength of the strong UV line C shown in Fig. 10a is temperature independent, and it is assigned to a delocalized excitation involving electron transfer from a nearest neighbor anion. The weak lines A and A' are assigned to the $A_{1g}(4d^{10}) \rightarrow T_{2g}(4d^9 5s)$ and $A_{1g}(4d^{10}) \rightarrow E_g(4d^9 5s)$ transitions, respectively. They display very little strength at 1.2 K but grow rapidly with increasing temperature. The change is much faster than can be obtained from the occupation number effect in the T_{1u} resonant mode.

We find that the increase in optical strength of A and A' with temperature is identical to that found earlier for the increase in the dc dielectric constant produced by the appearance of a permanent dipole moment with increasing temperature. This latter change was shown[41] to be proportional to the population P_{off} in the off-center configuration. By letting $P_{on} = 1 - P_{off}$, both the UV (squares) and dielectric constant (dotted line) data can be compared directly with the value of P_{on} determined from the temperature dependence of the T_{1u} resonant and gap mode strengths (dashed line)[41]. These results are graphed in Fig. 10b. All three experimental probes consistently measure the same rapid change in the population of the on-center configuration. A new discovery is the strong temperature dependence of the Raman scattering. As temperature is increased, the scattering strength of the previously observed 16.1 cm^{-1} E_g mode decreases rapidly

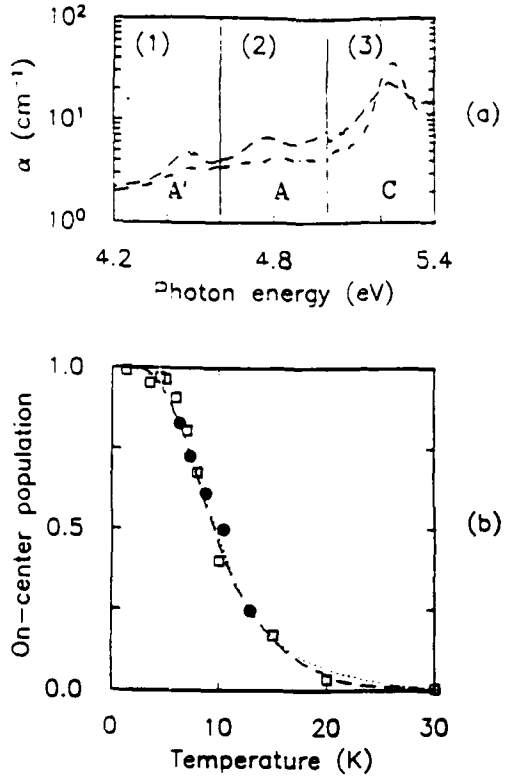

Figure. 10. (a) KI:Ag^+ UV absorption spectra. Dashed line, T = 50 K, dot-dashed line, T = 1.2 K. Silver concentration: (1) 2 x 10^{-2} mole %, (2) 2 x 10^{-3} mole %, (3) 5 x 10^{-5} mole %.
(b) Ag^+ on-center population temperature dependence, as determined by various measuring techniques. Dashed line, FIR resonant and gap mode data, Ref. 1. Dotted line, dielectric constant data , Ref. 2. Squares, UV absorption, A' mode, see text. Solid circles, Raman scattering, see text.

(see the solid circles in Fig. 10b), yet its center frequency stays nearly fixed. The temperature dependence of this Raman line is similar to that of the IR[40] and the optical features discussed above, but it takes on added importance because the E_g mode involves no motion of the Ag^+ ion.

The picture resulting from combining our experiments with Page's theoretical analysis is that of a nearly unstable low temperature defect-host configuration whose dynamics are explained within the harmonic approximation but whose population decreases dramatically with temperature. Thermal energy does not appear to modify the ground state dynamics. This behavior is in sharp contrast with that of "soft mode" systems, which also involve nearly unstable collective motion, but with dynamics that evolve continuously with temperature. Thus an approach fundamentally different than those for soft mode systems is required.

3. Conclusions

One way to explain the rapid transfer of population from one configuration to the other in with degeneracy. If the on-center configuration had a single state how much degeneracy would the

other configuration require to explain the experimental results? The answer is larger than 300 states! To see how this might come about let's first consider the thermodynamics of localized modes in perfect anharmonic crystals.

The production of these localized modes require the crystal energy to be increased over that found for the perfect crystal, but associated with the defect is crystal disorder which gives rise to an additional contribution to the entropy called configurational entropy, S_c. For a localized defect the Helmholtz free energy is given by

$$F = F_0 + nf - TS_c \ , \tag{3}$$

where F_0 describes the contribution from the perfect crystal, nf is the work done in creating n defects, and $-TS_c$ gives the contribution from the disorder. Minimizing the free energy with respect to the number of defects n for the limit where $n << N$ gives

$$n \approx N \exp(-f/k_B T) \ . \tag{4}$$

For the strongly localized mode limit the number of these modes present at any temperature is given by Eq. (4) with

$$f = \Delta\varepsilon - T\Delta s_v \tag{5}$$

where

$$\Delta\varepsilon = 3(\hbar\omega_l - \hbar\omega_m)/2 + pv \tag{6}$$

is the extra energy required to form this localized excitation at frequency ω_l from the band mode at an effective band edge frequency ω_m. There is a pv term here because the amplitude of the zero point motion at ω_l is larger than that at ω_m with the difference in the zero point volumes equal to v. In general, $\Delta s_v = s_l - s_m$ is the change in the vibrational entropy because of the energy change in the highest frequency mode but at low temperatures this term is zero.

The configurational entropy for the local mode case can be estimated as follows: Let V_d be the volume associated with a single localized mode in a crystal of volume V. The number of possible places where the mode can appear is (V/V_d) which is assumed to be a large macroscopic number, hence

$$S_c \approx k_B \ln (V/V_d)! \ / \ [(V/V_d) - n]! \ n! \tag{7}$$

and for the limit that $n << (V/V_d) \sim N$, the number of sites in the crystal then

$$n \approx N \exp(-\Delta\varepsilon/k_B T) \ . \tag{8}$$

At T = 0 K the local mode is not present; instead the highest frequency plane wave mode occurs at frequency ω_m. Equation (4) also shows that the number of anharmonic defects at low temperatures will be small since $f/k_B T >> 1$. It is expected that these modes can move from site to site so that the lattice can recover the translational symmetry once destroyed.

If the crystal contains defects then anharmonic localized modes can exist at T = 0 by appearing at the defect site. However, since these modes are mobile in the perfect lattice then at

some temperature T, the localized mode can be released from the defect site and move through the lattice. Since the mode can move in any direction in k space there are a large number of closely spaced levels in this second configuration, i.e., it has a large degeneracy.

For the particular case of KI:Ag^+ the release of a large amplitude localized breathing mode into the lattice would not only account for the large number of states in the second configuration but also with the large amplitude mode removed, the Ag^+ ion would occupy a larger volume cell hence cell with the possibility of acquiring an off center equilibrium position. Hence, it now appears that the occurrence of rapid temperature dependences in defect signatures such as the optical properties of "harmonic-like" vibrational modes at low temperatures may result from localized anharmonic modes being released into the lattice.

F. Publications, Reports and Theses (1990-92)

(Note: A ⊕ in front of the publication indicates that the work was supported by ARO.)

⊕ "Generalized Lyddane-Sachs-Teller Relation and Disordered Solids," A. J. Sievers and J. B. Page, Physical Review B **41**, 3455 (1990).

⊕ "Far Infrared Sphere Resonance in Isolated Superconducting Particles," T. W. Noh, S. G. Kaplan and A. J. Sievers, Physical Review B **41**, 307 (1990).

"Low Frequency Excitation Spectra of High T_c Superconductors," A. J. Sievers, T. W. Noh and S. G. Kaplan, **Phonons '89**, Proceedings of the Third Internatiuonal Conference on Phonon Physics, S. Hunklinger, W. Ludwig and G. Weiss, eds.(World Scientific, Singapore, 1990), Vol. 1, p. 237.

"Pulsed Laser Deposition of High T_c Superconducting Thin Films," S. E. Russek, B. H. Moeckly, R. A. Buhrman, J. T. McWhirter, A. J. Sievers, M. G. Norton, L. A. Tietz and B. Carter, Materials Research Society Symposium Proceedings **169**, 204, (1990).

"Hydrogen Adsorption on the βN covered W(100) Surface: An Infrared Study of the W-H Stretch," D. M. Riffe and A. J. Sievers, Physical Review B **41**, 3406 (1990).

"Infrared Diffuse Reflectivity Study of High T_c Superconductors," A. Rosenberg, A. S. Barker, T. W. Noh, T. Ohsaka and A. J. Sievers, Physical Review B **41**, 7213 (1990).

"IR study of (H,Be)-, (D,Be)- and (Li,Be)-acceptor complexes in silicon," R. E. Peale, K. Muro and A. J. Sievers, Physical Review B **41**, 5881 (1990).

"Far Infrared Absorption by Small Silver Particles in Gelatin," R. P. Devaty and A. J. Sievers, Physical Review B **41**, 7421 (1990).

⊕ "Persistent IR Spectral Hole Burning in Chalcogenide Glasses", S. P. Love and A. J. Sievers, J. of Luminescence **45**, 58 (1990).

⊕ "Optical and Mechanical Properties of Zinc Sulphide Diamond Composites," L. A. Xue, D. S. Farquar, R. Raj, T. W. Noh and A. J. Sievers, Acta Metall. Mater. **38**, 1743 (1990).

⊕ "On the Optical Response of a Disordered Solid with Restricted Size," A. J. Sievers and J. B. Page, Physical Review B **41**, 12 562 (1990).

⊕ "Persistent Infrared Spectral Hole Burning of Impurity Vibrational Modes in Chalcogenide Glasses", S. P. Love and A. J. Sievers, in *Transport, Correlation and Structural Defects*, Advances in Disordered Semiconductors, Vol. III, F. Fritzsche, ed., (World Scientific Publishing Co., Singapore, 1990), p. 27.

⊕ "Far IR Investigation of the Generalized Lyddane-Sachs-Teller Relation Using ZnS:diamond Composites," S. A. FitzGerald, T. W. Noh, A, J, Sievers, L. A. Xue and Y. Tzou, Phys. Rev. B **42**, 5469 (1990).

⊕ "Effect of Network Topology on Low Temperature Relaxation in Ge-As-Se Glasses as Probed By Persistent Infrared Spectral Hole Burning," S. P. Love, A. J. Sievers, B. L. Halfpap and S. M. Lindsay, Phys. Rev. Lett. **65**, 1792 (1990).

⊕ "Persistent Infrared Spectral Hole Burning," A. J. Sievers, Optics and Photonics **1**, No. 12, 53 (1990).

⊕ "IR Specroscopic Study of the Dressed Rotations of CN^- isotopes in Alkali Halide Crystals," C. E. Mungan, R. C. Spitzer, J. P. Sethna and A. J. Sievers, Phys. Rev. B **43**, 43 (1991).

⊕ "Intrinsic Localized Modes in a Monatomic Lattice with Weakly Anharmonic Nearest Neighbor Force Constants," S. R. Bickham and A. J. Sievers, Phys. Rev. B **43**, 2339 (1991).

⊕ "A Generalized Lyddane-Sachs-Teller Relation for Solids and Liquids," A. J. Sievers and J. B. Page, Infrared Physics **32**, 425 (1991).

⊕ "Four-Wave Mixing in the Far Infrared from Free Carriers in n-type InSb," R. M. Hart, G. A. Rodríguez and A. J. Sievers, Optics Letters **16**, 1511 (1991).

⊕ "Observation of Coherent Synchrotron Radiation at the Cornell Linac," E. B. Blum, U. Happek and A. J. Sievers, Nucl. Instrum. Methods Phys. Res., Sect. A, **307**, 568 (1991).

⊕ "Prediction and Observation of Pocket Vibrational Modes in Crystals," K. W. Sandusky, J. B. Page, A. Rosenberg, C. E. Mungan and A. J. Sievers, Phys. Rev. Lett. **67**, 871 (1991).

⊕ "A Generalized Lyddane-Sachs-Teller Relation for Solids and Liquids," A. J. Sievers and J. B. Page, Infrared Physics **32**, 425 (1991).

⊕ "Time Resolved Spectroscopy with Fourier Transform Spectrometers: Maintaining the Fellgett Advantage," J. T. McWhirter and A. J. Sievers, Applied Spectroscopy **45**, 1391 (1991).

⊕ "Persistent Infrared Spectral Hole Burning of NO_2^- Ions in Alkali Halide Crystals: I Principle and Satellite Hole Generation," W. P. Ambrose, J. P. Sethna and A. J. Sievers, J. Chem. Phys. **95**, 8816, (1991).

⊕ "Raman Scattering of KI:Ag^+: Exploration of a Nearly Unstable Defect-Lattice Configuration," H. Fleurent, W. Joosen, J. B. Page, A. J. Sievers, J. T. McWhirter, A. Bouwen and D. Schoemaker, "Radiation Effects and Defects in Solids" **119**, 577 (1991).

"Self-Consistency Conditions for the Effective Medium Approximation in Composite Materials," T. W. Noh, P. H. Song and A. J. Sievers, Physical Review B **43**, 5459 (1991).

⊕ "Observation of Coherent Transition Radiation," U. Happek, A. J. Sievers and E. B. Blum, Phys. Rev. Letters **67**, 2962 (1991).

"Sulfur-Hydrogen Donor Complexes in Silicon", R. E. Peale, K. Muro, and A. J. Sievers, in Proceedings of the Fourth International Conference on Shallow Impurities in Semiconductors, Materials Science Forum, editor Gordon Davies (Trans Tech Publications, Switzerland, 1990) Vols. 65-66 pp. 151-156.

"Self-Consistency Conditions for the Effective Medium Approximation in Composite Materials," T. W. Noh, P. H. Song and A. J. Sievers, Physical Review B **43**, 5459 (1991).

⊕ "Persistent IR Hole Burning in Crystals and Glasses," A. J. Sievers, J. of Luminescence **53**, 199 (1992).

⊕ "Persistent IR Spectral Hole-Burning of the Fundamental Stretching Mode of SH^- in Alkali Halides," C. E. Mungan and A. J. Sievers, J. Optical Society of America B **9**, 746 (1992).

⊕ "Vibrational Stark Effect for Matrix Isolated CN^- Molecules," R. C. Spitzer, A. J. Sievers and R. H. Silsbee, J. Optical Society of America B**10**, 714 (1992).

⊕ "Persistent Infrared Spectral Hole Burning of NO_2^- and NO_3^- Ions in Alkali Halide Crystals: II Spectral Changes Far from the Burn Frequency," W. P. Ambrose and A. J. Sievers, J. Optical Society of America B **9**, 753 (1992).

⊕ "Persistent Infrared Spectral Hole Burning of Tb^{3+} in the Glass-like Mixed Crystal $Ba_{1-x-y}La_xTb_yF_{2+x+y}$," S. P. Love, C. E. Mungan, A. J. Sievers and J. Campbell, J. Optical Society of America B **9**, 794 (1992).

⊕ "Numerical Measurements of the Shape and Dispersion Relation for Moving One–Dimensional Anharmonic Localized Modes," S. R. Bickham, A. J. Sievers, and S. Takeno, Phys. Rev. B **45**, 10344 (1992).

"Far Infrared Transmission of Superconducting K_xC_{60} Films," S. A. FitzGerald, S. G. Kaplan, A. Rosenberg A. J. Sievers and R. A. S. McMordie, Phys. Rev. B **45**, 10165 (1992).

⊕ "Stress Dependence of the Pocket Gap Modes in $KI:Ag^+$," A. Rosenberg, C. E. Mungan, A. J. Sievers, K. W. Sandusky and J. B. Page, Phs. Rev. B **46**, 11 507 (1992).

Reports

⊕ "Persistent IR Spectral Hole Burning of Tb3+ in the Glass-like Mixed Crystal $Ba_{1-x-y}La_xTb_yF_{2+x+y}$," S. P. Love, A. J. Sievers and J. A. Campbell, Bull. Amer. Phys. Soc. **35**, 548 (1990).

⊕ "Four-Wave-Mixing in the Far Infrared From Free Carriers in n-InSb." G. A. Rodríguez, R. M. Hart, A. Rosenberg, and A. J. Sievers, Bull. Amer. Phys. Soc. **36**, 453 (1991).

⊕ "Energy Transfer Between UV Generated Defects and IR Vibrational Modes of the CN^- Ion in Alkali Halide Crystals." J. T. McWhirter, U Happek and A. J. Sievers, Bull. Amer.

Phys. Soc. **36**, 841 (1991).

⊕ "Resonant Enhancement of Far Infrared Four-Wave-Mixing by Magnetoplasmons in n-InSb." R. M. Hart, G. A. Rodríguez and A. J. Sievers, Bull. Amer. Phys. Soc. **36**, 453 (1991).

"Antiferromagnetic Resonance in R_2CuO_4." S. G. Kaplan, T. W. Noh, A. J. Sievers, S–W. Cheong, Z. Fisk, Bull. Amer. Phys. Soc. **36**, 881 (1991).

⊕ "Simulations of Intrinsic Localized Modes in a 2-D Anharmonic Lattice. S. R. Bickham and A. J. Sievers, Bull. Amer. Phys. Soc. **36**, 919 (1991).

⊕ "Vibrational Relaxation of Diatomic Molecular Defects: Saturation Experiments on HS^- in Alkali Halide Hosts." U. Happek, J.T. McWhirter, C.E. Mungan, and A.J. Sievers, Bull. Amer. Phys. Soc. **36**, 918 (1991).

⊕ "Isotope Dependence of IR Localized Modes of CN^- in Potassium Halide Crystals." C.E. Mungan, R.C. Spitzer, J.P. Sethna, A.J. Sievers, Bull. Amer. Phys. Soc. **36**, 842 (1991).

⊕ "Crystalline and Glass-like FIR Properties Exhibited by Mixed Crystals of $(CaF_2)_{1-x}:(LaF_3)_x$." S. A. Fitzgerld, T. W. Noh, J. A Campbell, A. J. Sievers, Bull. Amer. Phys. Soc. **36**, 1022 (1991).

⊕ "Anomalous Isotope Effect for the Gap Mode in KI:Ag+, a Nearly Unstable Defect System." A. Rosenberg, C. E. Mungan and A. J. Sievers, Bull. Amer. Phys. Soc. **36**, 919 (1991).

⊕ (invited paper) "Persistent Infrared Spectral Hole Burning in Chalcogenide Glasses "— The Effects of Network Connectivity on Low–Temperature Relaxation. S. P. Love, Bull. Amer. Phys. Soc. **36**, 998 (1991).

"Glass-Like FIR Properties Exhibited by Air-glass Aerogels," B. B. Plapp, S. A. Fitzgerald, M. H.-W. Chan, A. J. Sievers, Bull. Amer. Phys. Soc. **37**, 397 (1992).

⊕ "Far Infrared Transmission of Superconducting K_xC_{60} Films," S. G. Kaplan, S. A. Fitzgerald, A. Rosenberg and A. J. Sievers, Bull. Amer. Phys. Soc. **37**, 714 (1992).

⊕ Glass Like FIR Properties Exhibited by Mixed Crystals of CaF_2, SrF_2 and BaF_2 Doped with LaF_3," S. A. Fitzgerald, J. A Campbell, A. J. Sievers, Bull. Amer. Phys. Soc. **37**, 235 (1992).

⊕ "Temperature Dependence of Dephasing Times in Chalcogenide Glasses," R. Till, A.J. Sievers, Bull. Amer. Phys. Soc. **37**, 237 (1992).

⊕ "Behavior of the KI:Ag^+ Far-Infrared Modes Under Uniaxial Stress," A. Rosenberg and A.J. Sievers, Bull. Amer. Phys. Soc. **37**, 489 (1992).

⊕ "Multi-librational Decay Hypothesis for the Stretching Modes of SH^- and OH^- in Alkali Halide Hosts," C.E. Mungan, U. Happek and A.J. Sievers, Bull. Amer. Phys. Soc. **37**, 721 (1992).

⊕ "Defect-Defect Energy Transfer Between Ionized Color Centers and the CN^- Ion in KBr," J. T. McWhirter, U. Happek, A.J. Sievers, Bull. Amer. Phys. Soc. **37**, 721 (1992).

⊕ "Experiments on the Energy Relaxation of the OH^- Stretching Mode in Alkali Halide Hosts," U. Happek, C.E. Mungan, and A.J. Sievers, Bull. Amer. Phys. Soc. **37**, 721 (1992)..

⊕ "Numerical Measurements of the Shape and Dispersion Relation for Moving One–Dimensional Anharmonic Localized Modes," S. R. Bickham, A. J. Sievers, and S. Takeno, Phys. Rev. B **45**, 10344 (1992).

⊕ "Numerical Measurements of the Shape and Dispersion Relation for Moving 1-D Anharmonic Localized Modes," S.R. Bickham, S.Takeno and A.J. Sievers, Bull. Amer. Phys. Soc. **37**, 490 (1992).

Theses

"IR Studies of Chemnical Splittings, Triplet Levels and Tunneling States at Electronic Defects in Silicon," R. E. Peale, Ph. D. Thesis, Cornell University (1990).

⊕ "Persistent Infrared Spectral Hole Burning Studies of Chalcogenide Glasses and Other Disordered Semiconductors," S. P. Love, Ph. D. Thesis, Cornell University (1991).

⊕ "Non-Resonant UV Pumping of IR Vibrational Fluorescence from CN^- in Alkali Halides," J. T. McWhirter, Ph. D. Thesis, Cornell University (1991).

⊕ "Intensity Dependent Cyclotron Resonance in a GaAs:AlGaAs Two Dimensional Electron Gas," Gerardo Rodriguez, Ph. D. Thesis, Cornell University (1991).

⊕ "Nonlinear Magnetooptics of Semiconductors in the Far Infrared," R. M. Hart, Ph. D. Thesis, Cornell University (1991).

⊕ "Far-Infrared Studies of a Thermally Unstable Lattice Defect System," A. Rosenberg, Ph. D. Thesis, Cornell University (1993).

G. Participating scientific personnel

S. R. Bickham, graduate student
J. T. McWhirter, graduate student
C. E. Mungan, graduate student
S. P. Love, graduate student
A. Rosenberg, graduate student
Gerardo Rodriguez, graduate student
R. M. Hart, graduate student
J. Engholm, graduate student

Dr. Uwe Happek, postdoc
Dr. Rainer Till, postdoc
Dr. T. W. Noh, postdoc
Dr. Sergey Kiselev, postdoc

Dr. John Campbell, visiting scientist

III. REFERENCES

1. P. H. Lee and L. S. Skolnick, Appl. Phys. Lett. **10**, 303 (1967).
2. A. Szabo, Phys. Rev. B **11**, 4512 (1975).
3. For a review see A. J. Sievers and W. E. Moerner in *Persistent Spectral Hole Burning: Science and Applications*, W. E. Moerner, ed. (Springer-Verlag, Berlin 1988), Chapter 6.
4. S. P. Love and A. J. Sievers, Chem. Phys. Lett. **153**, 379 (1988).
5. S. P. Love and A. J. Sievers, Bull. Am. Phys. Soc. **33**, 784 (1988).
6. S. P. Love and A. J. Sievers, *Proceedings of the 7th International Conference on Dynamical Processes in Excited States of Solids*, J. Luminescence **45**, 58 (1990).
7. R. Frerichs, J. Opt. Soc. Am. **43**, 1153 (1953).
8. For many excellent reviews, see *Optical Linewidths in Glasses*, M. J. Weber, ed., J. Luminescence **36**, 179-329 (1987).
9. P. M. Selzer, D. L. Huber, D. S. Hamilton, W. M. Yen, and M. J. Weber, Phys. Rev. Lett. **36**, 813 (1976).
10. J. Hegarty and W. M. Yen, Phys. Rev. Lett. **43**, 1126 (1979).
11. D. L. Huber, J. Non-Cryst. Solids **51**, 241 (1982).
12. S. K. Lyo and R. Orbach, Phys. Rev. B **29**, 2300 (1984).
13. I. S. Osad'ko and A. A. Shtygashev, J. Luminescence **36**, 315 (1987).
14. R. Silbey and K. Kassner, J. Luminescence **36**, 283 (1987).
15. J. C. Phillips, J. Non-Cryst. Solids **34**, 153 (1979).
16. M. F. Thorpe, J. Non-Cryst. Solids **57**, 355 (1983).
17. H. He and M. F. Thorpe, Phys. Rev. Lett. **54**, 2107 (1985).
18. S. Feng and M. F. Thorpe, Phys. Rev. B **31**, 276 (1985).
19. J. M. Hayes, R. Jankowiak, and G. J. Small in *Persistent Spectral Hole Burning: Science and Applications*, W. E. Moerner, ed. (Springer-Verlag, Berlin 1988), Chapter 5.
20. R. M. Macfarlane and R. M. Shelby in *Persistent Spectral Hole Burning: Science and pplications*, W. E. Moerner, ed. (Springer-Verlag, Berlin 1988), Chapter 4.
21. S. P. Love, et al., Phys. Rev. Letters **65**, 1792 (1990) .
22. P. W. Anderson , B. I. Halperin, and C. M. Varma, Philos. Mag. **25**, 1 (1971).
23. W. A. Phillips, J. Low Temp. Phys. **7**, 351 (1972).
24. D. G. Cahill and R. O. Pohl, Phys. Rev. B **39**, 10477 (1989).

25. S. P. Love, C. E. Mungan, A. J. Sievers and J. Cambell, J. Optical Society of America B (1992).
26. L. E. Erickson, Phys. Rev. B **19**, 4412 (1979).
27. R. M. Macfarlane et al., Phys. Rev. B **29**, 2390 (1984).
28. R. M. Shelby, Phys. Rev. B **21**, 5004 (1980).
29. W. P. Ambrose and A. J. Sievers, J. Optical Society of America B (1992).
30. W. P. Ambrose and A. J. Sievers, Chem. Phys. Lett. **147**, 608 (1988).
31. W. P. Ambrose and A. J. Sievers, Phys. Rev. B **38**, 10170 (1988).
32. A. J. Sievers and S. Takeno, Phys. Rev. Lett. **61**, 970 (1988).
33. S. Takeno and A. J. Sievers, Solid State Commun. **67**, 1023 (1988),
34 S. Takeno, K. Kisoda, and A. J. Sievers, Prog. Theor. Phys. Suppl. No.**94**, 242 (1988).
35. R. Bourbonnais and R. Maynard, Phys. Rev. Lett. **64**, 1397 (1990); R. Bourbonnais, Ph.D. Thesis, L'Universite Joseph Fourier, Grenoble, 1989, unpublished.
36. V. M. Burlakov, S. A. Kiselev and V. N. Pyrkov, Solid State Commun. **74**, 327 (1990); Phys. Rev. B **42**, 4921 (1990).
37. A. S. Barker and A. J. Sievers, Rev. Mod. Phys. **47**, Suppl. No. 2, Fall 1975.
38. J. B. Page, Phys. Rev. B **41**, 7835 (1990).
39. S. R. Bickham and A. J. Sievers, Phys., Rev. B **43**, 2339 (1991).
40. A. J. Sievers and L. H. Greene, Phys. Rev. Lett. **52**, 1234 (1984).
41. S. B. Hearon and A. J. Sievers, Phys. Rev. B **30**, 4853 (1984).
42. K. Fussgänger, phys. stat. sol. 34, 157 (1969) and phys. stat. sol **36**, 645 (1969).
43. J. B. Page, et al., Phys. Rev. Lett. 63, 1837 (1989).